WILEY | Hindawi

Research Article

Analytical Solution of Fractional Oldroyd-B Fluid via Fluctuating Duct

Ying Qing Song,[1] Aamir Farooq,[2] Muhammad Kamran [ID],[3] Sadique Rehman,[4] Muhammad Tamoor,[5,6] Rewayat Khan,[2] Asfand Fahad [ID],[7] and Muhammad Imran Qureshi [ID][7]

[1]*School of Science, Hunan City University, Yiyang 413000, China*
[2]*Department of Mathematics, Abbottabad University of Science and Technology, Havelian 22500, Pakistan*
[3]*Department of Mathematics, COMSATS University Islamabad, Wah Campus, Islamabad 47040, Pakistan*
[4]*Department of Pure and Applied Mathematics, University of Haripur, Haripur, KPK, Haripur, Pakistan*
[5]*Key Laboratory of Green Process and Engineering, Institute of Process Engineering, Chinese Academy of Sciences, Beijing 100190, China*
[6]*University of Chinese Academy of Sciences, Beijing 100049, China*
[7]*Department of Mathematics, COMSATS University Islamabad, Vehari Campus, Vehari 61100, Pakistan*

Correspondence should be addressed to Muhammad Imran Qureshi; imranqureshi18@gmail.com

This investigation focuses on the mixed initial boundary value problem with Caputo fractional derivatives. The studied pour an incompressible fractionalized Oldroyd-B fluid prompted by fluctuating rectangular tube. The explicit expression of the velocity field and shear stresses for the fractional model are obtained by utilizing the integral transforms, i.e., double finite Fourier sine transform and Laplace transform. Furthermore, the confirmation of the analytical solutions is also analyzed by utilizing the Tzou's and Stehfest's algorithms in the tabular form. In limited cases, ordinary Oldroyd-B fluid similar solutions and classical Maxwell and fractional Maxwell fluid are derived. The flow field's graphs with the influences of relevant parameters are also mentioned.

1. Introduction

The liquids which change their viscosity under force to either more liquid or solid are famous. These liquids are known as non-Newtonian fluids. The understanding can be improved by studying such types of fluids. A French physicist and engineer along with a mathematician named (Anglo-Irish, Claude-Louis Navier, and George Gabriel Stokes) described fluid flow through its environment. After it, these equations are known by their names like the Navier–Stokes equations. Navier–Stokes equations could describe the form and presentation of non-Newtonian fluids' flow quite well. These were proved useful in various areas of science and engineering. Petroleum engineers reveal how oil flows from well or pipe using mathematical modeling exactly in the same way as biomedical investigators for blood flow Non-Newtonian fluids have gained prominence because of their many uses in commerce and architecture, as well as medicine.

The non-Newtonian behavior understanding is generally more complicated than the Newtonian one. According to Hartnett and Kostic [1], in non-Newtonian fluids, the theoretical predictions yield low estimates of the heat transfer under laminar flow conditions. The motion of non-Newtonian fluid in containers is a very functional issue in dynamics. First, Stokes [2] presented the precise result of oscillatory motion in a classical linearly viscous fluid. Rajagopal [3] answered the models of non-Newtonian fluids in regards to their motion. Rajagopal and Bhatnagar [4] studied the Oldroyd-B fluid solutions in Bessel function for torsional and the longitudinal oscillations of an enormously

lengthy dowel. Mahmood et al. [5] used Laplace and finite Hankel transform and acquired the exact velocity's solutions and sinusoidal shear stress corresponding to second-grade fluid's flow. Hayat et al. [6] found out the five particular results used for the problems of an Oldroyd-B fluid, i.e., (i) Stokes problem, (ii) modified Stokes problem, (iii) the time-periodic Poiseuille flow due to an oscillating pressure gradient, (iv) the nonperiodic flows between two boundaries, and (v) symmetric flow with an arbitrary initial velocity.

In the last decades, fractional calculus (FC) underwent intensive research and development [7]. The working and comprehension of artificial and characteristic frameworks require the conventional derivative and integral which are significant for innovation experts. The derivative operators and calculus integral can be characterized by fractional calculus which is the field of math wherein the fractional powers are utilized instead of integer powers. Therefore, noninteger derivatives are portrayed by some memory impacts that are imparted to various materials such as polymers and viscoelastic materials and furthermore its uses in anomalous diffusions. By [8], we obtained exact solutions using an expansion theorem of Steklov for flows satisfying no-slip boundary conditions. Waters and King [9] evaluated the exact solution with the Laplace transform. They investigated that the velocity sketches intensely subject to the flexible parameters and fluctuates approximately on their central position. Wood [10] studied start-up helical flows for Oldroyd-B in straight tubes of the annular and rounded cross-section. They added that the fluid is originally at rest for completing the process of the solution.

Electromagnetic, viscoelasticity, fluid mechanics, electrochemistry, biological population models, optics, and signal processing are just a few of the engineering and science fields where fractional calculus is used. Ray et al. [11] discussed fractional calculus as a modeling tool for engineering and physical advancements that are defined vigorously by fractional differential equations. Systems that require precise damping modeling used fractional derivative models to accurately model it. Various analytical and numerical techniques, as well as their presentations to new complications, have been projected in these fields [12, 13].

Researches in fluid flow problems are present in terms of fractional derivatives. They had observed the influence of fractional parameters on the flow profiles [14, 15]. They referred to the obtained governing equations as fractional partial differential equations. Moreover, through discrete Laplace transform and Fourier transform along with some well-known special functions, they got precise results [16]. Few scholars considered Oldroyd-B fluid for various models in terms of fractional derivatives. Fetecau et al. [17, 18] solved Stokes's first problem of the velocity profile and the related tangential tension parallel to an Oldroyd-B fluid flow above abruptly stimulated smooth bowl analytically. Fetecau et al. [19] investigated the tangential pressures and velocity field between two perpendicular walls in the trembling flow of Oldroyd-B fluid by continuously accelerating a plate. They obtained the exact solution with the utilization of the Fourier transform method. Different geometries exist in different types of solutions. In industry, ducts are normally used for

managing different flows. Therefore, as a prime process part in industrial units, it gained high importance. The rotational flow of fractional Oldroyd-B fluid in cylindrical domains was studied in [20, 21]. Fetecau and Fetecau [22] used a rectangular cross-sectional channel and introduced precise results for two different kinds of trembling flows of an Oldroyd-B fluid. Nazar et al. [23] determined sine oscillations of the rectangular tube through studying the mandatory time-period to reach the steady-state. Riaz et al. [21] used fractional derivatives and investigated the rotating flow of an Oldroyd-B fluid caused by an infinite circular tube with a continuous couple. Ghada and Ahmed [24] find out the trembling flow of broad Oldroyd-B fluid by studying the analytic solution and the flow of fluid was in the oscillating rectangular tube.

Furthermore, Wang et al. [25] used an extended rectangular cross-sectional tube and investigated the vibratory flow of Maxwell fluid. The exact solution's singularities and appropriate expressions of velocity and phase variation were studied clearly. Sun et al. [26] used an isosceles right triangular cross-sectional lengthy tube and modeled the vibratory flow of the Maxwell fluid. They obtained analytical terms for the flow compelled by the periodic pressure gradient. Farooq et al. [27] studied the generalized Maxwell fluid flow with magnetic and porous factors via quadrilateral duct. Sultan et al. [28] found out the trembling magneto-hydrodynamic (MHD) flow of Oldroyd-B fluid through analytic solution in a permeable rectangular cross-section. Some studies related to time-fractional derivatives have obtained interesting results of such flow problems [29–35]. This paper aims to express the oscillatory motion of an Oldroyd-B fluid through a rectangular duct. The unsteady boundary layer equations of Oldroyd-B fluid are formulated. Then, the exact solutions are derived for the comprehensive Oldroyd-B fluid through integral transform. More precisely, the researchers want to know the relation of the vibratory motion of the fractionalized Oldroyd-B fluid by discovering the shear stress and velocity motion, and the first "time" derivative of the velocity is taken "zero" as its extra condition to simplify the model at time $t = 0$. Furthermore, the effects and features are graphically represented that are relevant to velocity field's parameters.

The remainder of this article is designed in such a way that, after the introduction, the statement of the problem is discussed in Section 2. In Section 3, we presented the exact solution of related velocity field and tangential stresses specific to Oldroyd-B fluid inside a vibratory rectangular tube with fractional derivatives. Section 4 discusses limited cases of the fractional Oldroyd-B fluid. The graphical results and the derived exact solutions compared with numerical results are investigated in Section 5. The conclusion of the paper is presented in Section 6. Also, see Table 1 for the dimension of the physical parameters.

2. Statement of the Problem

This paper considers the incompressible fractional Oldroyd-B fluid (FOBF) in the quadrilateral tube in Figure 1. The dimensions of the sides are $\mathscr{X} = 0$, $\mathscr{X} = d$, $\mathscr{Y} = 0$, and

TABLE 1: Nomenclature.

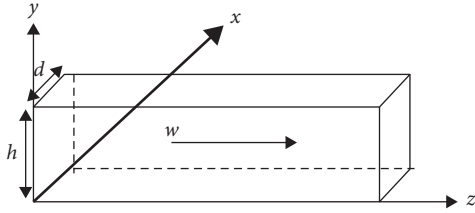| Symbols	Quantity
Ω	$\mathscr{Z}$-direction velocity (ms^{-1})
λ_1	Relaxation time (s)
λ_2	Retardation time (s)
μ	Dynamic viscosity (kgm^{-1}s^{-1})
U_0	Amplitude (m)
ω	Angular frequency (rads^{-1})
d	Length of duct (m)
h	Height of duct (m)
ρ	Density of fluid (kgm^{-3})
α, β	Fractional parameters
LT	Laplace transform
V	Velocity of fluid (ms^{-1})
S	Tangential stress (Nm^{-2} or Pa)
p	Pressure (kgm^{-1}s^{-2})

FIGURE 1: Flow through rectangular duct.

$\mathscr{Y} = h$. At time $t = 0^+$, the tube starts to vibrate along $\mathscr{Z}$-axis. Due to these oscillations, an oscillatory motion in fluid gets started inside along the duct's boundary. The considered velocity field and tangential stress are as follows:

$$\mathbf{V}(\mathscr{X}, \mathscr{Y}, \mathscr{Z}) = \mathbf{\Omega}(\mathscr{X}, \mathscr{Y}, t)\mathbf{k} = (0, 0, \Omega)\mathbf{S} = \mathbf{S}(\mathscr{X}, \mathscr{Y}, t), \tag{1}$$

where **k** is the unit vector aiming in $\mathscr{Z}$-direction. Remember the first **B** kinematic tensor can be given from Rivlin-Ericksen as

$$\mathbf{B} := \nabla\mathbf{V} + (\nabla\mathbf{V})^{\dagger}, \tag{2}$$

where $\dagger$ represents the operation transpose. The stress tensor **T** is

$$\mathbf{T} := -p\mathbf{I} + \mathbf{S}. \tag{3}$$

This equation indicates p, **I**, and **S** which are the hydrostatic pressure, identity tensor, and extra stress tensor, respectively. The extra stress tensor [36] can be written as by the following relation:

$$(1 + \lambda_1\mathscr{D}_t)[\mathbf{S}] = \mu(1 + \lambda_2\mathscr{D}_t)[\mathbf{B}]. \tag{4}$$

In (4) $\mu > 0$, λ_1 and λ_2 are the dynamic viscosity, relaxation time, and retardation time, respectively. The operator denotes the Oldroyd derivative [36] $\mathscr{D}_t$ and is given below

$$\mathscr{D}_t[\mathbf{S}] := \partial_t\mathbf{S} + (\mathbf{V}.\nabla)\mathbf{S} + (\nabla\mathbf{V})\mathbf{S} + \mathbf{S}(\nabla\mathbf{V})^{\dagger}. \tag{5}$$

Furthermore, the initial conditions for the considered fluid flow are

$$\mathbf{S}(\mathscr{X}, \mathscr{Y}, 0) = 0 = \partial_t\mathbf{S}(\mathscr{X}, \mathscr{Y}, 0). \tag{6}$$

The assumed governing equations for an incompressible fluid system are

$$\nabla.\mathbf{V} = 0,$$
$$\rho[\partial_t\mathbf{V} + (\mathbf{V}.\nabla)\mathbf{V}] = \nabla.\mathbf{S}, \tag{7}$$

while $\rho > o$; for ease, body strength and pressure gradient are overlooked.

2.1. Flow Problem.

Firstly, the researchers carefully weighed the flow of Oldroyd-B fluid and the possible constitutive equations for it. Then, after the exact modification, the researchers found out the desired results for the fluids' flow. (1) satisfies the equation of continuity, i.e., (6). While (1), (2) and (4), (3), together with the initial conditions, i.e., (5), we can get for all $t > 0$,

$$S_{xx} = S_{yy} = 0, \tag{8}$$

$$(1 + \lambda_1\partial_t)S_{xz} = \mu(1 + \lambda_2\partial_t)\partial_{\mathscr{X}}\Omega, \tag{9}$$

$$(1 + \lambda_1\partial_t)S_{yz} = \mu(1 + \lambda_2\partial_t)\partial_{\mathscr{Y}}\Omega. \tag{10}$$

Using the same procedure [28] and with the help of (1) and (8)–(10), we can reduce (7) to

$$\rho(1 + \lambda_1\partial_t)\partial_t\Omega = \mu(1 + \lambda_2\partial_t)(\partial^2_{\mathscr{X}}\Omega + \partial^2_{\mathscr{Y}}\Omega). \tag{11}$$

The appropriate conditions are

$$\Omega(\mathscr{X}, \mathscr{Y}, 0) = \partial_t\Omega(\mathscr{X}, \mathscr{Y}, 0) = 0,$$
$$\Omega(0, \mathscr{Y}, t) = \Omega(d, \mathscr{Y}, t) = \Omega(\mathscr{X}, 0, t) = \Omega(\mathscr{X}, h, t)$$
$$= U_0 H(t)\cos(wt), \quad t > 0,$$
$$\Omega(\mathscr{X}, \mathscr{Y}, 0) = \partial_t\Omega(\mathscr{X}, \mathscr{Y}, 0) = 0,$$
$$\Omega(0, \mathscr{Y}, t) = \Omega(d, \mathscr{Y}, t) = \Omega(\mathscr{X}, 0, t) = \Omega(\mathscr{X}, h, t)$$
$$= U_0\sin(wt), \quad t > 0, \tag{12}$$

where U_0 is the amplitude, $H(t)$ is a unit step function, and ω is the velocity frequency of edge. While forgetting the fractional Oldroyd-B fluid flow equations, the researchers need to change the inner time derivatives (11) with left-sided Caputo fractional time derivatives ∂_t^{α} and ∂_t^{β} for $0 < \alpha \leq \beta < 1$, and it can be diverted into the model with the same original boundary conditions accurately,

$$\rho(1 + \lambda_1^{\alpha}\partial_t^{\alpha})\partial_t\Omega = \mu(1 + \lambda_2^{\beta}\partial_t^{\beta})(\partial^2_{\mathscr{X}}\Omega + \partial^2_{\mathscr{Y}}\Omega), \tag{13}$$

where the Caputo's fractional derivative [13] is

$$D_t^{\wp}f(t) = \frac{1}{\Gamma(1 - \wp)}\int_0^t \frac{f'(\tau)}{(t - \tau)^{\wp}}d\tau, \quad 0 \leq \wp < 1, \tag{14}$$

and $\Gamma(.)$ is the gamma function.

To balance the dimension of (13), we bring into the power α and β on λ_1 and λ_2, respectively. Moreover, we will use the following dimensionless quantities to normalize the (13).

$$\hat{\mathcal{X}} = \frac{\mathcal{X}}{d},$$

$$\hat{\mathcal{Y}} = \frac{\mathcal{Y}}{h},$$

$$\hat{\Omega} = \frac{\Omega}{u_0},$$

$$\hat{t} = \frac{\mu t}{\rho\, dh},$$

$$\hat{\lambda_1} = \frac{\mu\lambda_1}{\rho\, dh}, \tag{15}$$

$$\hat{\lambda_2} = \frac{\mu\lambda_2}{\rho\, dh},$$

$$\hat{\omega} = \frac{\rho\, dh\, \omega}{\mu},$$

$$\gamma = \frac{d}{h}.$$

With the help of the above dimensionless quantities and dropping the hats sign, the (13) will become

$$(1 + \lambda_1^\alpha \partial_t^\alpha)\partial_t \Omega = \frac{1}{\gamma}\left(1 + \lambda_2^\beta \partial_t^\beta\right)\left(\partial_{\mathcal{X}}^2 \Omega + \gamma^2 \partial_{\mathcal{Y}}^2 \Omega\right), \tag{16}$$

$$\Omega(\mathcal{X}, \mathcal{Y}, 0) = \partial_t \Omega(\mathcal{X}, \mathcal{Y}, 0) = 0,$$
$$\Omega(0, \mathcal{Y}, t) = \Omega(1, \mathcal{Y}, t) = \Omega(\mathcal{X}, 0, t), \tag{17}$$
$$\Omega(\mathcal{X}, 1, t) = H(t)\cos(wt), \quad t > 0,$$

or

$$\Omega(\mathcal{X}, \mathcal{Y}, 0) = \partial_t \Omega(\mathcal{X}, \mathcal{Y}, 0) = 0,$$
$$\Omega(0, \mathcal{Y}, t) = \Omega(1, \mathcal{Y}, t) = \Omega(\mathcal{X}, 0, t), \tag{18}$$
$$\Omega(\mathcal{X}, 1, t) = \sin(wt), \quad t > 0.$$

3. Solution of Velocity Profile

3.1. $\Omega(0, \mathcal{Y}, t) = \Omega(1, \mathcal{Y}, t) = \Omega(\mathcal{X}, 0, t) \quad = \Omega(\mathcal{X}, 1, t)$ $= \sin(\omega t)$. Operating $\sin(\alpha_l \mathcal{X})\sin(\beta_n \mathcal{Y})$ on (16), then integrating concerned $\mathcal{X}$ and $\mathcal{Y}$ over $[0, 1] \times [0, 1]$, and utilizing the transmuted original and boundary conditions (18), we will get

$$(1 + \lambda_1^\alpha D_t^\alpha)\partial_t \Omega_{lp}(t) + \frac{\lambda_{lp}^2}{\gamma}\left(1 + \lambda_2^\beta D_t^\beta\right)\Omega_{lp}(t)$$
$$= \frac{a_{lp}\lambda_{lp}^2}{\gamma}\left(1 + \lambda_2^\beta D_t^\beta\right)\sin(wt), \tag{19}$$

where $\alpha_l = l\pi$, $\beta_p = p\pi$, $a_{lp} = [1 - (-1)]^l[1 - (-1)^p]/\alpha_l\beta_p$, and $\lambda_{lp}^2 = \alpha_l^2 + \gamma^2\beta_p^2$, and

$$\Omega_{lp}(t) = \int_0^1 \int_0^1 \Omega(\mathcal{X}, \mathcal{Y}, t)\sin(\alpha_l \mathcal{X})\sin(\beta_p \mathcal{Y})d\mathcal{X}d\mathcal{Y},$$
$$l, p = 1, 2, 3 \ldots, \tag{20}$$

is the binary Fourier alteration of $\Omega(\mathcal{X}, \mathcal{Y}, t)$.

By applying Laplace transformation and appropriate transform conditions on equation (15) we will get $\overline{\Omega}_{lp}(q)$ as

$$\overline{\Omega}_{lp}(q) = \frac{a_{lp}\lambda_{lp}^2}{\gamma}\frac{\omega}{q^2 + \omega^2}\frac{1 + \lambda_2^\beta q^\beta}{q + \lambda_1^\alpha q^{\alpha+1} + \left(\lambda_{lp}^2/\gamma\right)\left(1 + \lambda_2^\beta q^\beta\right)}, \tag{21}$$

or

$$\overline{\Omega}_{lp}(q) = \frac{a_{lp}\lambda_{lp}^2}{\gamma}\frac{\omega}{q^2 + \omega^2}\overline{F}_{lp}(q), \tag{22}$$

where

$$\overline{F}_{lp}(q) = \frac{1 + \lambda_2^\beta q^\beta}{q + \lambda_1^\alpha q^{\alpha+1} + \left(\lambda_{lp}^2/\gamma\right)\left(1 + \lambda_2^\beta q^\beta\right)}, \tag{23}$$

which can be written as

$$\overline{F}_{lp}(q) = \frac{\gamma}{\lambda_{lp}^2} - \frac{1 + \lambda_1^\alpha q^\alpha}{1 + \lambda_1^\alpha q^\alpha + \left(\lambda_{lp}^2/\gamma\right)\left(1 + \lambda_2^\beta q^\beta\right)q^{-1}}\frac{\gamma}{\lambda_{lp}^2}, \tag{24}$$

and the Laplace transform of $\Omega_{lp}(t)$ is $\overline{\Omega}_{lp}(q) = \int_0^\infty \Omega_{lp}(t)e^{-qt}dt$ (22) which becomes

$$\overline{\Omega}_{lp}(q) = a_{lp}\frac{\omega}{q^2 + \omega^2} - a_{lp}\omega\frac{q}{q^2 + \omega^2}$$
$$\times \frac{q^{-1} + \lambda_1^\alpha q^{\alpha-1}}{1 + \lambda_1^\alpha q^\alpha + \left(\lambda_{lp}^2/\gamma\right)\left(1 + \lambda_2^\beta q^\beta\right)q^{-1}}. \tag{25}$$

So it is denoted by

$$\overline{F}(q) = \frac{q\left(q^{-1} + \lambda_1^\alpha q^{\alpha-1}\right)}{q^2 + \omega^2}, \tag{26}$$

and the inverse LT of the $\overline{F}(q)$ is

$$f(t) = L^{-1}\{\overline{F}(q)\} = \frac{\lambda_1^\alpha}{\Gamma(1-\alpha)}\int_0^t \frac{\cos(\omega t)}{(t-\psi)^\alpha}d\psi$$
$$+ \frac{\sin(\omega t)}{\omega}, \quad 0 < \alpha < 1. \tag{27}$$

Now, we consider the function

$$\overline{A}_{lp}(q) = \frac{1}{1 + \lambda_1^\alpha q^\alpha + \left(\lambda_{lp}^2/\gamma\right)\left(1 + \lambda_2^\beta q^\beta\right)q^{-1}}. \tag{28}$$

With the help of $1/(x + a) = \sum_{k=0}^\infty (-1)^k (x^k/a^{k+1})$, $(a + b)^k = \sum_{m=0}^k (k!/(k-m)!m!)a^m b^{(k-m)}$, the expression for $\overline{A}_{lp}(q)$ can be written as

$$\overline{A}_{lp}(q) = \sum_{k=0}^{\infty}\sum_{n=0}^{k}\left(\frac{-\lambda_{lp}^2}{\gamma}\right)^k \frac{k!\lambda_2^{\beta n}}{n!(k-n)!\lambda_1^{\alpha(k+1)}} \times \frac{q^{\beta n-k}}{(q^\alpha+\lambda_1^{-\alpha})^{k+1}}. \tag{29}$$

The inverse LT of the expression (29) is

$$a_{lp}(t) = \sum_{k=0}^{\infty}\sum_{n=0}^{k}\left(\frac{-\lambda_{lp}^2}{\gamma}\right)^k \frac{k!\lambda_2^{\beta n}}{n!(k-n)!\lambda_1^{\alpha(k+1)}} \tag{30}$$
$$\times G_{\alpha,\beta n-k,k+1}\left(-\lambda_1^{-\alpha},t\right),$$

where $G_{e,f,g}(h,t)$ is the generalized G-function as defined in [37].

$$G_{e,f,g}(h,t) = \sum_{i=0}^{\infty}\frac{d^i\Gamma(r+i)}{\Gamma(r)\Gamma(1+i)}\frac{t^{(r+i)a-b-1}}{\Gamma[(r+i)a-b]}. \tag{31}$$

The transformed velocity can be rewritten as

$$\overline{\Omega}_{lp}(q) = a_{lp}\frac{\omega}{q^2+\omega^2} - a_{lp}\omega\overline{F}(q)\overline{A}_{lp}(q). \tag{32}$$

The inverse LT of the (32) is

$$\Omega_{lp}(t) = a_{lp}\sin(\omega t) - a_{lp}\omega\big(f(t)*a_{lp}(t)\big), \tag{33}$$

where $f(t)*a_{lp}(t) = \int_o^t f(t-q)a_{lp}(t)dq$ denotes the convolution product. Taking the inverse Fourier transform to (33) and using the formula [38], the velocity field for sin oscillation is

$$\Omega_s(\mathcal{X},\mathcal{Y},t) = \sin(\omega t) - 4\sum_{l,p=1}^{\infty}a_{lp}\omega\sin(\alpha_l\mathcal{X})\sin(\beta_p\mathcal{Y})$$
$$\times\big(f(t)*a_{lp}(t)\big). \tag{34}$$

It can be rewritten as

$$\Omega_s(\mathcal{X},\mathcal{Y},t) = \sin(\omega t) - 16\omega\sum_{l,p=0}^{\infty}\frac{\sin((2l+1)\pi\mathcal{X})}{(2l+1)\pi}$$
$$\times\frac{\sin((2p+1)\pi\mathcal{X})}{(2p+1)\pi} \tag{35}$$
$$\big(f(t)*a_{(2l+1)(2p+1)}(t)\big).$$

The dimensionless tangential stresses T_1 and T_2 associated with the fractional Oldroyd-B fluid in such motions are given by

$$\left(1+\lambda_1^\alpha D_t^\alpha\right)T_{1s}(\mathcal{X},\mathcal{Y},t) = \left(1+\lambda_2^\beta D_t^\beta\right)\partial_\mathcal{X}\Omega(\mathcal{X},\mathcal{Y},t), \tag{36}$$

$$\left(1+\lambda_1^\alpha D_t^\alpha\right)T_{2s}(\mathcal{X},\mathcal{Y},t) = \left(1+\lambda_2^\beta D_t^\beta\right)\partial_\mathcal{Y}\Omega(\mathcal{X},\mathcal{Y},t), \tag{37}$$

where $T_{1s} = dS_{xz}/\mu u_0$ and $T_{2s} = hS_{yz}/\mu u_0$.
Taking the Laplace transform of (36), we can get

$$\overline{T}_{1s}(\mathcal{X},\mathcal{Y},q) = \frac{1+\lambda_2^\beta q^\beta}{1+\lambda_1^\alpha q^\alpha}\partial_\mathcal{X}\overline{\Omega}_s(\mathcal{X},\mathcal{Y},q). \tag{38}$$

Rewrite (38) as

$$\overline{T}_{1s}(\mathcal{X},\mathcal{Y},q) = \left[1+\frac{\lambda_2^\beta}{\lambda_1^\alpha}\frac{q^\beta}{q^\alpha+\lambda_1^{-\alpha}} - \frac{q^\alpha}{q^\alpha+\lambda_1^{-\alpha}}\right]\times\partial_\mathcal{X}\overline{\Omega}(\mathcal{X},\mathcal{Y},q), \tag{39}$$

where

$$\overline{\Omega}(\mathcal{X},\mathcal{Y},q) = \frac{\omega}{q^2+\omega^2} - 16\omega\sum_{l,p=0}^{\infty}\frac{\sin((2l+1)\pi\mathcal{X})}{(2l+l)\pi}$$
$$\times\frac{\sin((2p+1)\pi\mathcal{Y})}{(2p+1)\pi} \tag{40}$$
$$\left(\overline{F}(q)\overline{A}_{(2l+1)(2p+1)}(q)\right).$$

Invoking $\partial_\mathcal{X}\overline{\Omega}(\mathcal{X},\mathcal{Y},t)$ in (40), we will get

$$\overline{T}_{1s}(\mathcal{X},\mathcal{Y},q) = \left[1+\frac{\lambda_2^\beta}{\lambda_1^\alpha}\frac{q^\beta}{q^\alpha+\lambda_1^{-\alpha}} - \frac{q^\alpha}{q^\alpha+\lambda_1^{-\alpha}}\right]$$
$$\times -16\omega\sum_{l,p=0}^{\infty}\cos((2l+1)\pi\mathcal{X})\frac{\sin((2p+1)\pi\mathcal{Y})}{(2p+1)\pi}$$
$$\times\left(\overline{F}(q)\overline{A}_{(2l+1)(2p+1)}(q)\right). \tag{41}$$

The inverse LT of the above relation is

$$T_{1s}(\mathcal{X},\mathcal{Y},t) = -16\sum_{l,p=0}^{\infty}\omega\cos((2l+1)\pi\mathcal{X})\frac{\sin((2p+1)\pi\mathcal{Y})}{(2p+1)\pi}$$
$$\times f(t)*a_{(2l+1)(2p+1)}(t) - \frac{16\lambda_r^\beta}{\lambda^\alpha}\sum_{l,p=0}^{\infty}\omega\cos$$
$$\cdot((2l+1)\pi\mathcal{X})\times\frac{\sin((2p+1)\pi\mathcal{Y})}{(2p+1)\pi}$$
$$\cdot f(t)*g(t)*a_{(2l+1)(2p+1)}(t)$$
$$+16\sum_{l,p=0}^{\infty}\omega\cos((2l+1)\pi\mathcal{X})\frac{\sin((2p+1)\pi\mathcal{Y})}{(2p+1)\pi}$$
$$\times f(t)*g(t)*a_{(2l+1)(2p+1)}(t). \tag{42}$$

where $g(t) = L^{-1}(q^\beta/q^\alpha+\lambda_1^{-\alpha}) = R_{\alpha,\beta}(-\lambda_1^{-\alpha},t)$, $h(t) = L^{-1}(q^\alpha/q^\alpha+\lambda_1^{-\alpha}) = H(t) - (1/\lambda_1^\alpha)R_{\alpha,0}(-\lambda_1^{-\alpha},t)$, and $R_{a,b}(e,f,t) = \sum_{p=0}^{\infty}e^p(t-f)^{(p+1)a-b-1}/\Gamma[(p+1)a-b]$.
Similarly, we can calculate T_{2s} from (37).

3.2. $\Omega(0,\mathcal{Y},t) = \Omega(1,\mathcal{Y},t) = \Omega(\mathcal{X},0,t) = \Omega(\mathcal{X},1,t) = H(t)\cos(\omega t)$. Operating $\sin(\alpha_l\mathcal{X})\sin(\beta_p\mathcal{Y})$ on (16), then integrating with respect to $\mathcal{X}$ and $\mathcal{Y}$ over $[0,1]\times[0,1]$, and

together with the transformed boundary conditions (17), we obtain

$$(1 + \lambda_1^\alpha D_t^\alpha)\partial_t \Omega_{lp}(t) + \frac{\lambda_{lp}^2}{\gamma}\left(1 + \lambda_2^\beta D_t^\beta\right)\Omega_{lp}(t)$$

$$= \frac{a_{lp}\lambda_{lp}^2}{\gamma}\left(1 + \lambda_2^\beta D_t^\beta\right)H(t)\cos(wt). \quad (43)$$

Now, taking the LT of (43) with an appropriate transform condition, we will obtain the expression for $\overline{\Omega}_{lp}(q)$ as

$$\overline{\Omega}_{lp}(q) = \frac{a_{lp}\lambda_{lp}^2}{\gamma}\frac{q}{q^2 + \omega^2}\frac{1 + \lambda_2^\beta q^\beta}{q + \lambda_1^\alpha q^{\alpha+1} + \left(\lambda_{lp}^2/\gamma\right)\left(1 + \lambda_2^\beta q^\beta\right)}, \quad (44)$$

or

$$\overline{\Omega}_{lp}(q) = \frac{a_{lp}\lambda_{lp}^2}{\gamma}\frac{q}{q^2 + \omega^2}\overline{F}_{lp}(q). \quad (45)$$

Putting $F_{lp}(q)$ in (45),

$$\overline{\Omega}_{lp}(q) = a_{lp}\frac{q}{q^2 + \omega^2} - a_{lp}\frac{q}{q^2 + \omega^2}$$

$$\times \frac{1 + \lambda_1^\alpha q^\alpha}{1 + \lambda_1^\alpha q^{\alpha+1} + \left(\lambda_{lp}^2/\gamma\right)\left(1 + \lambda_2^\beta q^\beta\right)q^{-1}}, \quad (46)$$

where $\overline{K}(q) = q(1 + \lambda_1^\alpha q^\alpha)/q^2 + \omega^2$, the inverse LT of the $\overline{K}(q)$ is

$$k(t) = L^{-1}\{\overline{K}(q)\} = \frac{\lambda_1^\alpha}{\Gamma(-\alpha)}\int_0^t \frac{\cos(\omega t)}{(t - \tau)^{\alpha+1}}\,d\tau$$

$$+ \cos(\omega t), \quad 0 < \alpha < 1. \quad (47)$$

Rewrite $\overline{\Omega}_{lp}(q)$,

$$\overline{\Omega}_{lp}(q) = a_{lp}\frac{q}{q^2 + \omega^2} - a_{lp}\overline{K}(q)\overline{A}_{lp}(q). \quad (48)$$

The inverse LT (48) is

$$\Omega_{lp}(t) = a_{lp}\cos(\omega t) - a_{lp}\left(k(t) * a_{lp}(t)\right), \quad (49)$$

where $k(t) * a_{lp}(t) = \int_0^t f(t - s)a_{lp}(t)\,ds$ denotes the convolution product of $k(t)$ and $a_{lp}(t)$. Taking the inverse Fourier alteration of (49) and utilizing the formula [38], the velocity profile is

$$\Omega_c(\mathcal{X}, \mathcal{Y}, t) = \cos(wt) - 4\sum_{l,p=1}^\infty a_{lp}\sin(\alpha_l\mathcal{X})\sin(\beta_p\mathcal{Y})$$

$$\times\left(k(t) * a_{lp}(t)\right). \quad (50)$$

Rewrite (50),

$$\Omega_c(\mathcal{X}, \mathcal{Y}, t) = \cos(wt) - 16\sum_{l,p=0}^\infty \frac{\sin((2l + 1)\pi\mathcal{X})}{(2l + 1)\pi}$$

$$\times\frac{\sin((2p + 1)\pi\mathcal{Y})}{(2p + 1)\pi}\left(k(t) * a_{(2l+1)(2p+1)}(t)\right). \quad (51)$$

Using the same technique as of the above section, we can find the tangential stresses under the forms:

$$T_{1c}(\mathcal{X}, \mathcal{Y}, t) = -16\sum_{l,p=0}^\infty \cos((2l + 1)\pi\mathcal{X})\frac{\sin((2p + 1)\pi\mathcal{Y})}{(2p + 1)\pi}$$

$$\times f(t) * a_{(2l+1)(2p+1)}(t)$$

$$- \frac{16\lambda_2^\beta}{\lambda_1^\alpha}\sum_{l,p=0}^\infty \cos((2l + 1)\pi\mathcal{X})$$

$$\times\frac{\sin((2p + 1)\pi\mathcal{Y})}{(2p + 1)\pi} f(t) * g(t) * a_{(2l+1)(2p+1)}(t)$$

$$+ 16\sum_{l,p=0}^\infty \cos((2l + 1)\pi\mathcal{X})\frac{\sin((2p + 1)\pi\mathcal{Y})}{(2p + 1)\pi}$$

$$\times f(t) * h(t) * a_{(2l+1)(2p+1)}(t). \quad (52)$$

Similarly, we can calculate T_{2c}.

4. Limiting Cases

4.1. Classical Oldroyd-B Fluid. Creating $\alpha \longrightarrow 1$ and $\beta \longrightarrow 1$ into (35), (42), (51), and (52), we can acquire a similar solution of the velocity distribution of both cases for trembling flows of an ordinary Oldroyd-B fluid. Thus, the velocity field and shear stresses decrease to

$$\Omega s(\mathcal{X}, \mathcal{Y}, t) = \sin(\omega t) - 16\omega\sum_{l,p=0}^\infty \frac{\sin((2l + 1)\pi\mathcal{X})}{(2l + 1)\pi}$$

$$\times\frac{\sin((2p + 1)\pi\mathcal{Y})}{(2p + 1)\pi}\left(f(t) * a_{(2l+1)(2p+1)}(t)\right),$$

$$\Omega_c(\mathcal{X}, \mathcal{Y}, t) = \cos(\omega t) - 16\sum_{l,p=0}^\infty \frac{\sin((2l + 1)\pi\mathcal{X})}{(2l + 1)\pi}$$

$$\times \frac{\sin((2p+1)\pi_Y)}{(2p+1)\pi}\left(k(t) * a_{(2l+1)(2p+1)}(t)\right),$$

$$T_{1s}(\mathcal{X},\mathcal{Y},t) = -16\sum_{l,p=0}^{\infty}\omega\cos((2l+1)\pi\mathcal{X})\times\frac{\sin((2p+1)\pi\overline{Y})}{(2p+1)\pi}f(t) * a_{(2l+1)(2p+1)}(t)$$

$$-\frac{16\lambda_r}{\lambda}\sum_{l,p=0}^{\infty}\omega\cos((2l+1)\pi\mathcal{X})\times\frac{\sin((2p+1)\pi\mathcal{Y})}{(2p+1)\pi}f(t) * h(t) * a_{(2l+1)(2p+1)}(t)$$

$$+16\sum_{l,p=0}^{\infty}\omega\cos((2l+1)\pi\mathcal{X})\frac{\sin((2p+1)\pi\mathcal{Y})}{(2p+1)\pi}\times f(t) * h(t) * a_{(2l+1)(2p+1)}(t),$$

$$T_{1c}(\mathcal{X},\mathcal{Y},t) = -16\sum_{l,p=0}^{\infty}\cos((2l+1)\pi\mathcal{X})\times\frac{\sin((2p+1)\pi\mathcal{Y})}{(2p+1)\pi}f(t) * a_{(2l+1)(2p+1)}(t)$$

$$-\frac{16\lambda_r}{\lambda}\sum_{l,p=0}^{\infty}\cos((2l+1)\pi\mathcal{X})\times\frac{\sin((2p+1)\pi\mathcal{Y})}{(2p+1)\pi}f(t) * h(t) * a_{(2l+1)(2p+1)}(t)$$

$$+16\sum_{l,p=0}^{\infty}\cos((2l+1)\pi\mathcal{X})\frac{\sin((2p+1)\pi\mathcal{Y})}{(2p+1)\pi}\times f(t) * h(t) * a_{(2l+1)(2p+1)}(t), \tag{53}$$

where $a_{lp}(t) = \sum_{k=0}^{\infty}\sum_{n=0}^{k}(-\lambda_{lp}^2/\gamma)^k$ $(k!(\lambda_2^n)/n!(k-n)!$ $\lambda_1^{(k+1)})G_{1,l-1,k+1}(-\lambda_1^{-1},t)$, $f(t) = \lambda_1\cos(\omega t) + (\sin(\omega t)/\omega)$, $k(t) = \lambda_1\cos(\omega t) + \lambda_1(H(t) - \omega\sin(\omega t))$, $\alpha = 1$, and $h(t) = L^{-1}(q/q + \lambda_1^{-1}) = H(t) - (1/\lambda_1)R_{1,0}(-\lambda_1^{-1},t)$.

4.2. Fractional Maxwell Fluid.

Making $\lambda_2 \longrightarrow 0$ into (35), (42), (51), and (52), then we can acquire both cases of identical solution of velocity dispersion and shear stress for generalized Maxwell fluid's flows [38]. Thus, the velocity field and shear stresses decrease to

$$\Omega_s(\mathcal{X},\mathcal{Y},t) = \sin(\omega t) - 16\omega\sum_{l,p=0}^{\infty}\frac{\sin((2l+1)\pi\mathcal{X})}{(2l+1)\pi}\times\frac{\sin((2p+1)\pi\mathcal{Y})}{(2p+1)\pi}\left(f(t) * a_{(2l+1)(2p+1)}(t)\right),$$

$$\Omega_c(\mathcal{X},\mathcal{Y},t) = \cos(\omega t) - 16\sum_{l,p=0}^{\infty}\frac{\sin((2l+1)\pi\mathcal{X})}{(2l+1)\pi}\times\frac{\sin((2p+1)\pi\mathcal{Y})}{(2p+1)\pi}\left(k(t) * a_{(2l+1)(2p+1)}(t)\right),$$

$$T_{1s}(\mathcal{X},\mathcal{X},t) = -16\sum_{l,p=0}^{\infty}\omega\cos((2m+1)\pi\mathcal{X})\times\frac{\sin((2p+1)\pi\mathcal{Y})}{(2p+1)\pi}f(t) * a_{(2l+1)(2p+1)}(t)$$

$$+16\sum_{l,p=0}^{\infty}\omega\cos((2l+1)\pi\mathcal{X})\frac{\sin((2p+1)\pi\mathcal{Y})}{(2p+1)\pi}f(t) * h(t) * a_{(2l+1)(2p+1)}(t),$$

$$T_{1c}(\mathcal{X},\mathcal{Y},t) = -16\sum_{l,p=0}^{\infty}\cos((2l+1)\pi\mathcal{X})\times\frac{\sin((2p+1)\pi\mathcal{Y})}{(2p+1)\pi}f(t) * a_{(2l+1)(2p+1)}(t)$$

$$+16\sum_{l,p=0}^{\infty}\cos((2l+1)\pi\mathcal{X})\frac{\sin((2p+1)\pi\mathcal{Y})}{(2p+1)\pi}f(t) * h(t) * a_{(2l+1)(2p+1)}(t), \tag{54}$$

where

$$a_{lp}(t) = \sum_{k=0}^{\infty}\left(\frac{-\lambda_{lp}^2}{\gamma}\right)^k\frac{1}{\lambda_1^{\alpha(k+1)}}G_{\alpha,-1,k+1}(-\lambda_1^{-\alpha},t). \tag{55}$$

4.3. Classical Maxwell Fluid.

Making $\lambda_2 \longrightarrow 0$ and $\alpha \longrightarrow 1$ into (35), (42), (51), and (52), we can acquire a similar solution of velocity distribution and shear stresses of both the cases for trembling flows of classical Maxwell fluid [23]. Thus, the velocity field and shear stresses decrease to
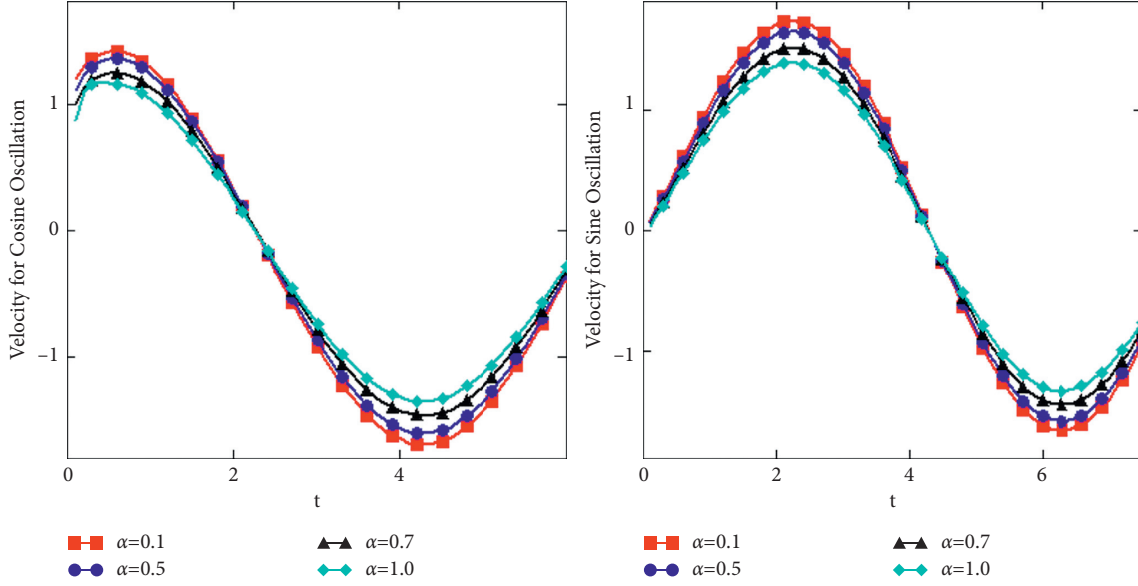
FIGURE 2: The variation of α for both the oscillations with $\omega = \pi/4$, $\lambda = 0.8$, $\lambda_r = 0.5$, $\beta = 0.8$, $\gamma = 2$, $\mathscr{X} = 0.45$, and $\mathscr{Y} = 0.1$.
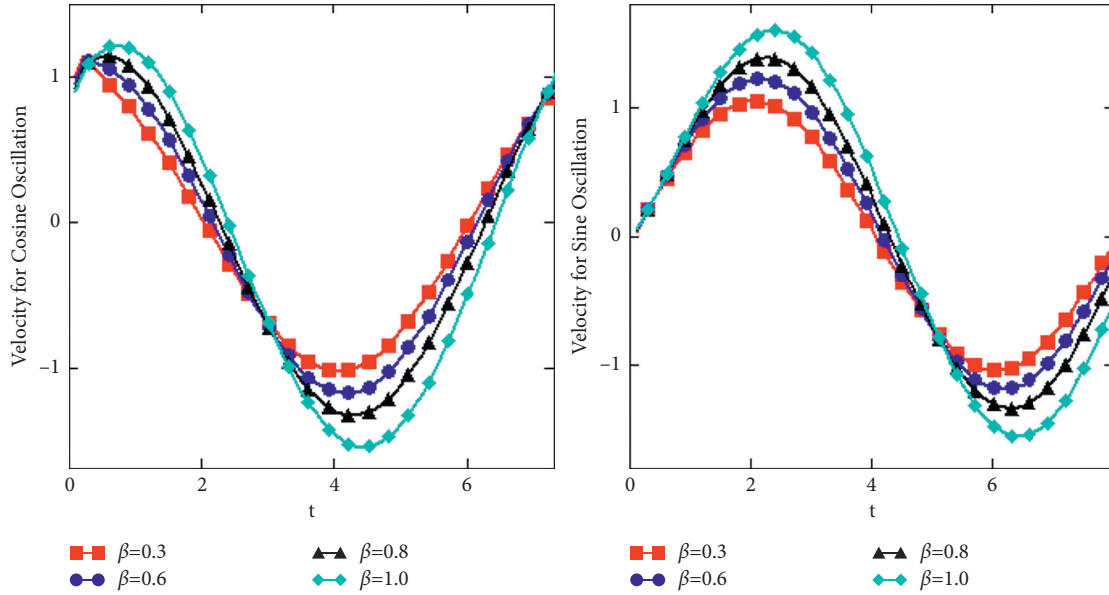

FIGURE 3: The variation of β for both the oscillations with $\omega = \pi/4$, $\lambda_1 = 0.8$, $\lambda_2 = 0.5$, $\alpha = 0.8$, $\gamma = 2$, $\mathscr{X} = 0.45$, and $\mathscr{Y} = 0.1$.

$$\Omega s(\mathscr{X}, \mathscr{Y}, t) = \sin(\omega t) - 16\omega \sum_{l,p=0}^{\infty} \frac{\sin((2l+1)\pi\mathscr{X})}{(2l+1)\pi} \times \frac{\sin((2p+1)\pi\mathscr{Y})}{(2p+1)\pi} \left(f(t) * a_{(2l+1)(2p+1)}(t) \right),$$

$$\Omega_c(\mathscr{X}, \mathscr{Y}, t) = \cos(\omega t) - 16 \sum_{l,p=0}^{\infty} \frac{\sin((2l+1)\pi\mathscr{X})}{(2l+1)\pi} \times \frac{\sin((2p+1)\pi\mathscr{Y})}{(2p+1)\pi} \left(k(t) * a_{(2l+1)(2p+1)}(t) \right),$$

$$T_{1s}(\mathscr{X}, \mathscr{Y}, t) = -16 \sum_{l,p=0}^{\infty} \omega \cos((2l+1)\pi\mathscr{X}) \times \frac{\sin((2p+1)\pi\mathscr{Y})}{(2p+1)\pi} f(t) * a_{(2l+1)(2p+1)}(t)$$
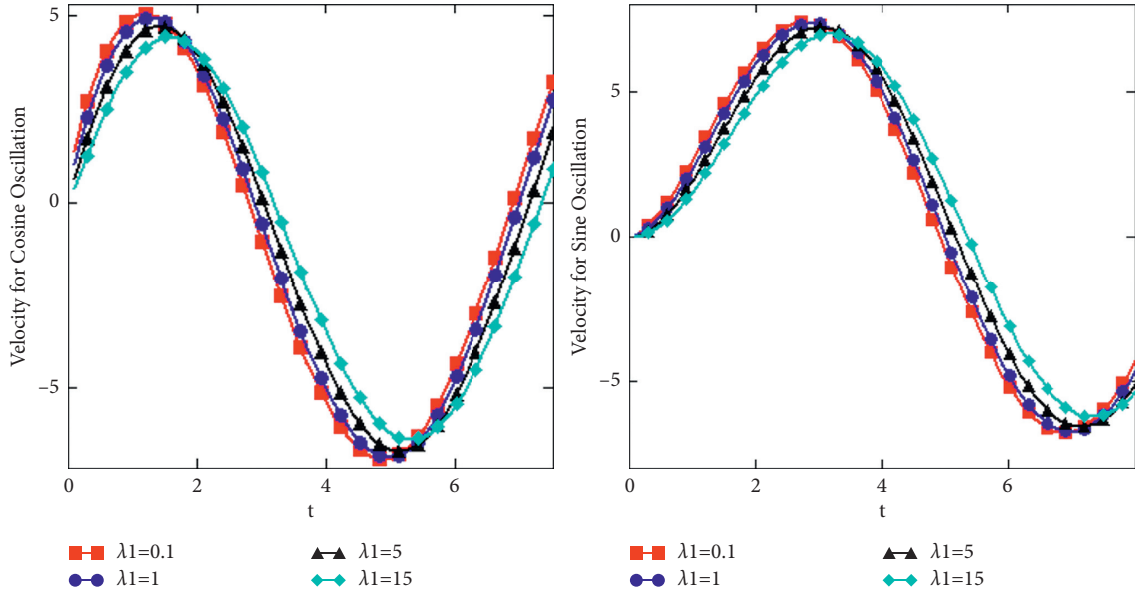
FIGURE 4: The variation of λ_1 for both the oscillations with $\omega = \pi/4$, $\alpha = 0.5$, $\lambda_2 = 0.07$, $\beta = 0.9$, $\gamma = 2$, $\mathcal{X} = 0.25$, and $\mathcal{Y} = 0.1$.
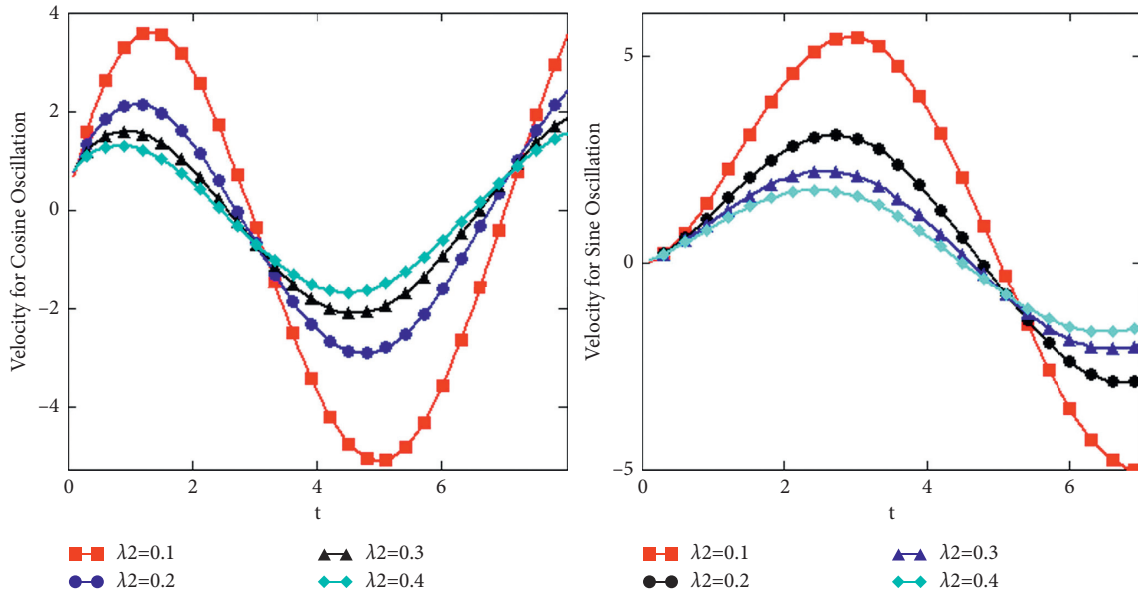

FIGURE 5: The variation of λ_2 for both the oscillations with $\omega = \pi/4$, $\lambda_1 = 5$, $\alpha = 0.5$, $\beta = 0.9$, $\gamma = 2$, $\mathcal{X} = 0.25$, and $\mathcal{Y} = 0.1$.

$$+ 16 \sum_{l,p=0}^{\infty} \omega \cos\left((2l+1)\pi\mathcal{X}\right) \frac{\sin\left((2p+1)\pi\mathcal{Y}\right)}{(2p+1)\pi} \times f(t) * h(t) * a_{(2l+1)(2p+1)}(t),$$

$$T_{1c}(\mathcal{X}, \mathcal{Y}, t) = -16 \sum_{l,p=0}^{\infty} \cos\left((2l+1)\pi\mathcal{X}\right) \times \frac{\sin\left((2p+1)\pi\mathcal{Y}\right)}{(2p+1)\pi} f(t) * a_{(2l+1)(2p+1)}(t)$$

$$+ 16 \sum_{l,p=0}^{\infty} \cos\left((2l+1)\pi\mathcal{X}\right) \frac{\sin\left((2p+1)\pi\mathcal{Y}\right)}{(2p+1)\pi} \times f(t) * h(t) * a_{(2l+1)(2p+1)}(t), \qquad (56)$$
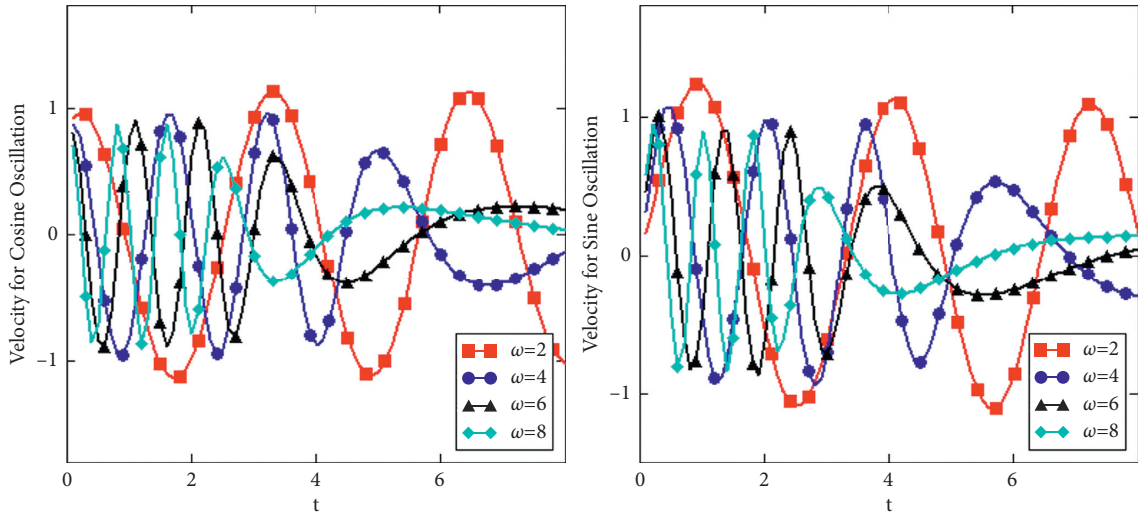
FIGURE 6: The variation of ω for both the oscillations with $\gamma = 2$, $\alpha = 0.5$, $\lambda_1 = 0.8$, $\beta = 0.9$, $\lambda_2 = 0.5$, $\mathcal{X} = 0.25$, and $\mathcal{Y} = 0.1$.
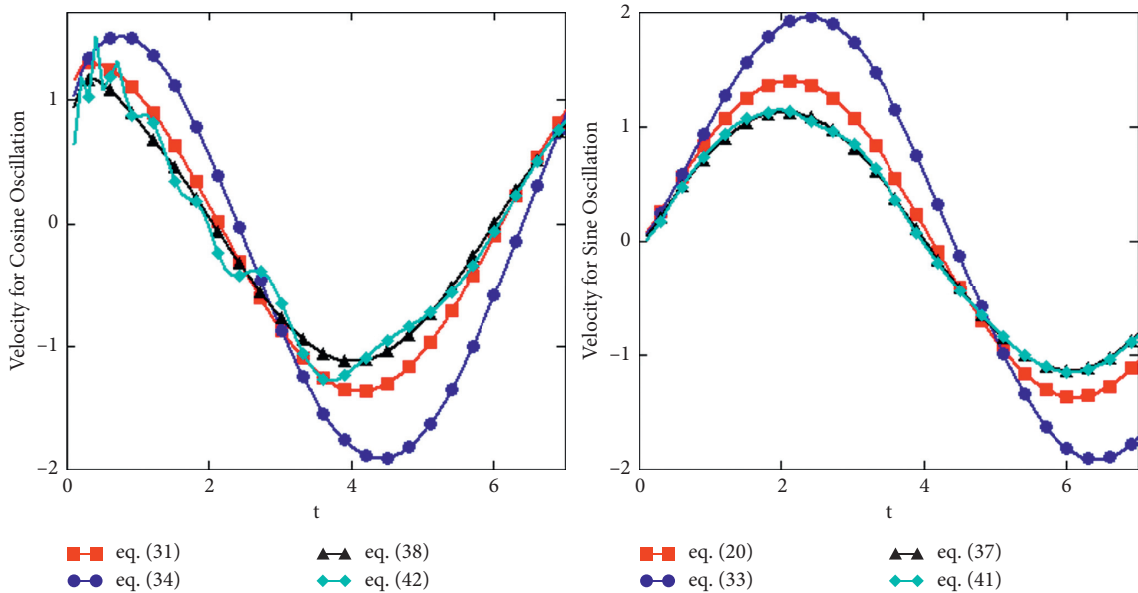

FIGURE 7: Velocity profiles of fractional Oldroyd-B fluid, classical Oldroyd-B fluid, fractional Maxwell fluid, and classical Maxwell fluid for both cos and sin.

where

$$a_{lp}(t) = \sum_{k=0}^{\infty} \left(\frac{-\lambda_{lp}^2}{\gamma} \right)^k \frac{1}{\lambda_1^{(k+1)}} G_{1,-1,k+1}\left(-\lambda_1^{-1}, t\right). \tag{57}$$

5. Numerical Results

In this section, we will give graphically results for the velocity and shear stresses profiles for the various parameters. Also, we will show a comparison between the analytical and numerical results in a tabular form. The numerical results were obtained by Stehfest's and Tzou's numerical inverse Laplace algorithms. The access of the various physical parameters for time is graphically presented in Figures 2 to 13.

In Figure 2, the researchers strategized the absolute values of the velocity field versus time. The given diagrams are strategized for four values of the fractional coefficient α. The velocity of the fluid decreases (absolute values) is observed as $\alpha \longrightarrow 1$ for the back and forth moment of both sine and cosine vibrations. In Figure 3, the researchers drew the consequences of the second fractional parameter β on the velocity field versus time. It was expected an opposite behavior concerning the first fractional parameter α and seen it comes true in the plot of Figure 3. In Figures 4 and 5, the effect of the relaxation parameter and the delay time on fluid motion is seen. From this figure, it is observed that its behavior is identical to that of a fractional parameter α, and when the fractional derivative parameter extends to 1 for the back and forth moment of both sine and cosine, the velocity
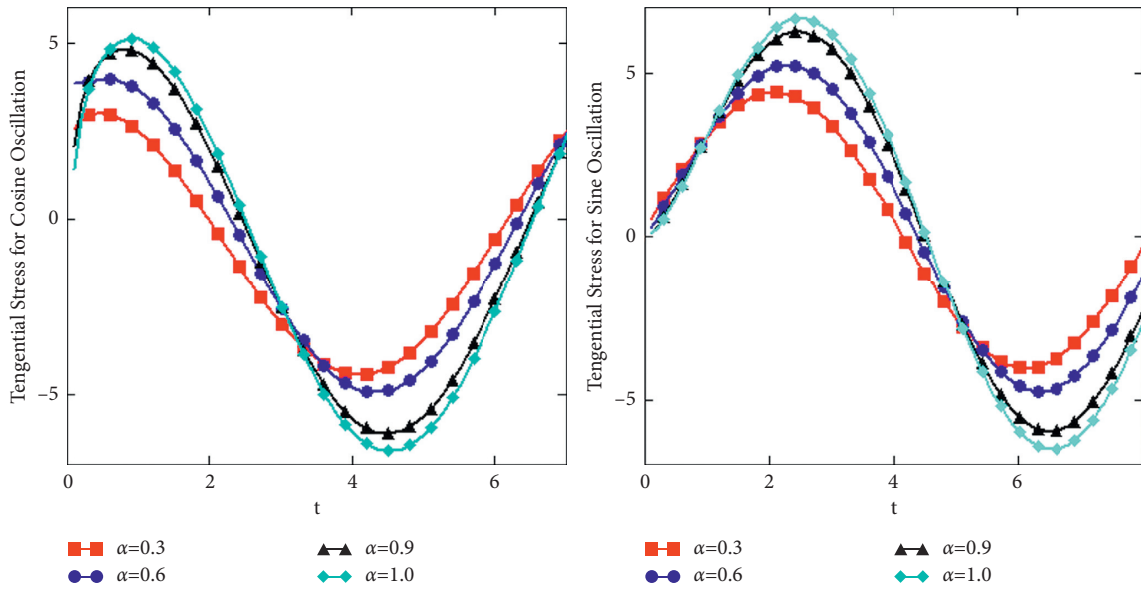
FIGURE 8: The variation of α for both the oscillations with $\omega = \pi/4$, $\lambda_1 = 0.8$, $\lambda_2 = 0.5$, $\beta = 0.8$, $\gamma = 2$, $\mathscr{X} = 0.55$, and $\mathscr{Y} = 0.15$.
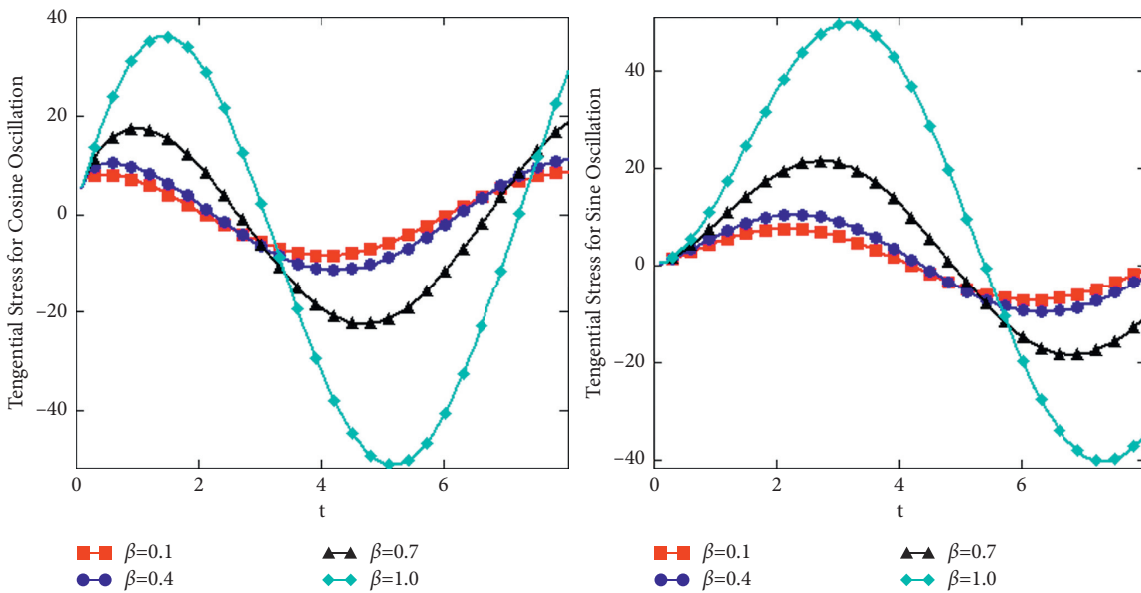

FIGURE 9: The variation of β for both the oscillations with $\omega = \pi/4$, $\lambda_1 = 0.08$, $\lambda_2 = 0.05$, $\alpha = 0.8$, $\gamma = 2$, $\mathscr{X} = 0.55$, and $\mathscr{Y} = 0.15$.

of the fluid reduces (nonabsolute values). Figure 6 exhibits the fluid factor w on the fluids flow. It shows the same behavior like Figures 2, 4, and 5, i.e., it describes that the fluid flow decreases with the enlargement of such parameter. The comparison of dimensionless velocities for fractional Oldroyd-B, ordinary Oldroyd-B, fractional Maxwell fluid, and ordinary Maxwell fluid is presented in Figure 7. It is clear that fractional Oldroyd-B fluid is the hastiest and fractional Maxwell fluid is the slowest in absolute values.

In Figure 8, the dimensionless shear stress versus t drew for various values of fractional coefficient α. The given diagrams are strategized for three values of the α. The stress on the fluid decreases for half interval of time, and the next half, it increases for sine oscillation because the standards of

fractional parameter α increase. Figure 9 is sketched to show the dimensionless shear stress versus t directed for various values of fractional coefficient β. It can be observed that the effect of parameter β on the fluid motion has an opposite behavior compared to parameter α. Figures 10 and 11 are showing the effects of relaxation and retardation time on fluid motion. They have the opposite effect on stress as expected due to the relation between the return of a perturbed system into equilibrium and delayed response to an applied force or stress. Figure 12 gives the impact of frequency factor w on the shear stress. From Figure 12, it is clearly sighted that shear stress of the fluid goes to decay due to the increase of w. The comparison of dimensionless shear stresses for fractional Oldroyd-B, ordinary Oldroyd-B,

FIGURE 10: The variation of λ_1 for both the oscillations with $\omega = \pi/4$, $\beta = 0.7$, $\lambda_2 = 0.1$, $\alpha = 0.2$, $\gamma = 2$, $\mathscr{X} = 0.55$, and $\mathscr{Y} = 0.15$.
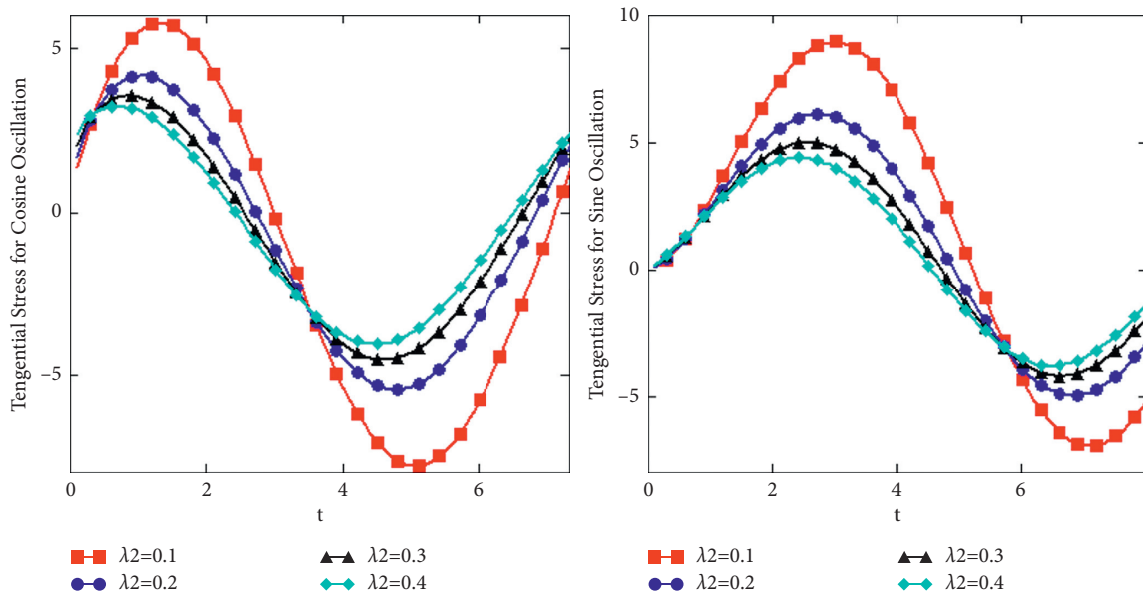
FIGURE 11: The variation of λ_2 for both the oscillations with $\omega = \pi/4$, $\beta = 0.7$, $\lambda_1 = 2$, $\alpha = 0.5$, $\gamma = 2$, $\mathscr{X} = 0.55$, and $\mathscr{Y} = 0.15$.

fractional Maxwell fluid, and ordinary Maxwell fluid is presented in Figure 13. From Figure 13, we noticed that the fractional parameter shows the increasing behavior for both the Oldroyd-B and Maxwell fluid as compared to the classical Oldroyd-B and Maxwell fluid.

It is clear from Tables 2 to 5 that the analytical solutions are nearly equal to the numerical results. The Stehfest's algorithm shows quite good agreement with our analytical solutions as compared to the numerical results obtained by Tzou's algorithm.
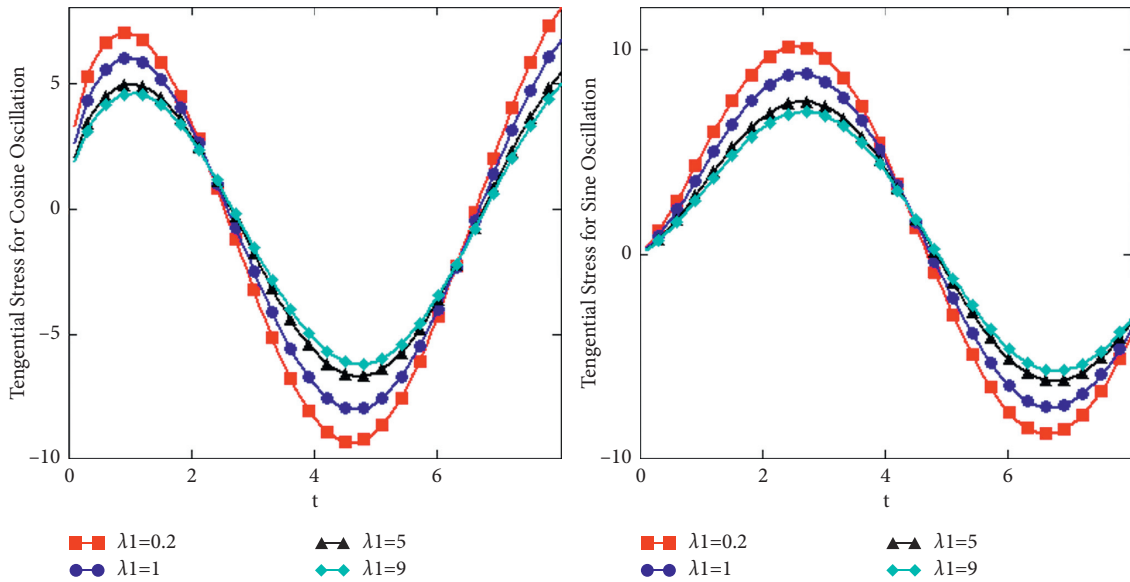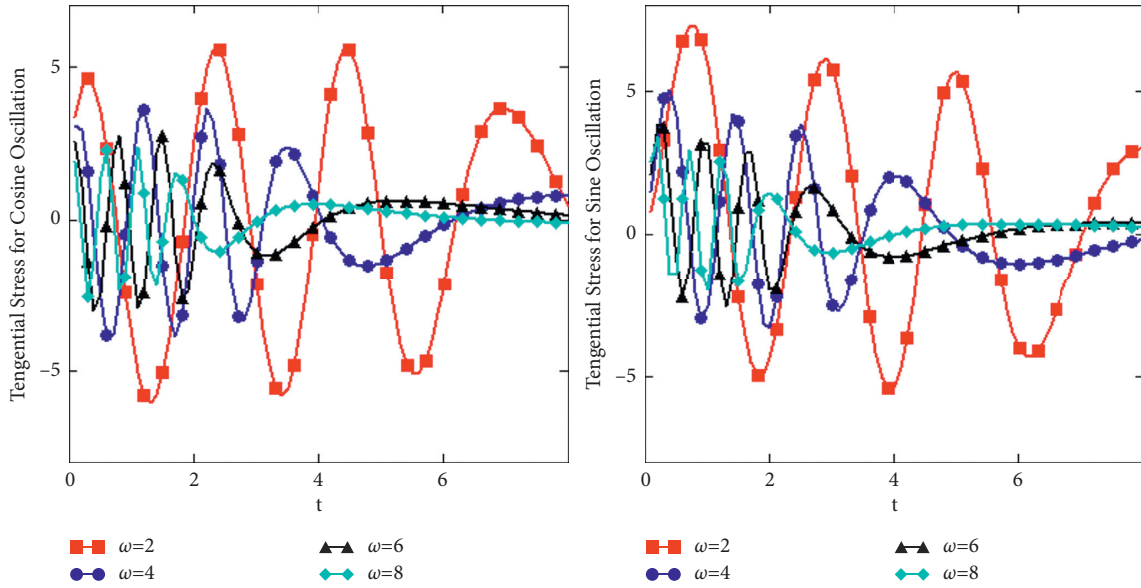
FIGURE 12: The variation of ω for both the oscillations with $\lambda_2 = 0.1$, $\beta = 0.7$, $\lambda_1 = 0.3$, $\alpha = 0.5$, $\gamma = 2$, $\mathscr{X} = 0.55$, and $\mathscr{Y} = 0.15$.
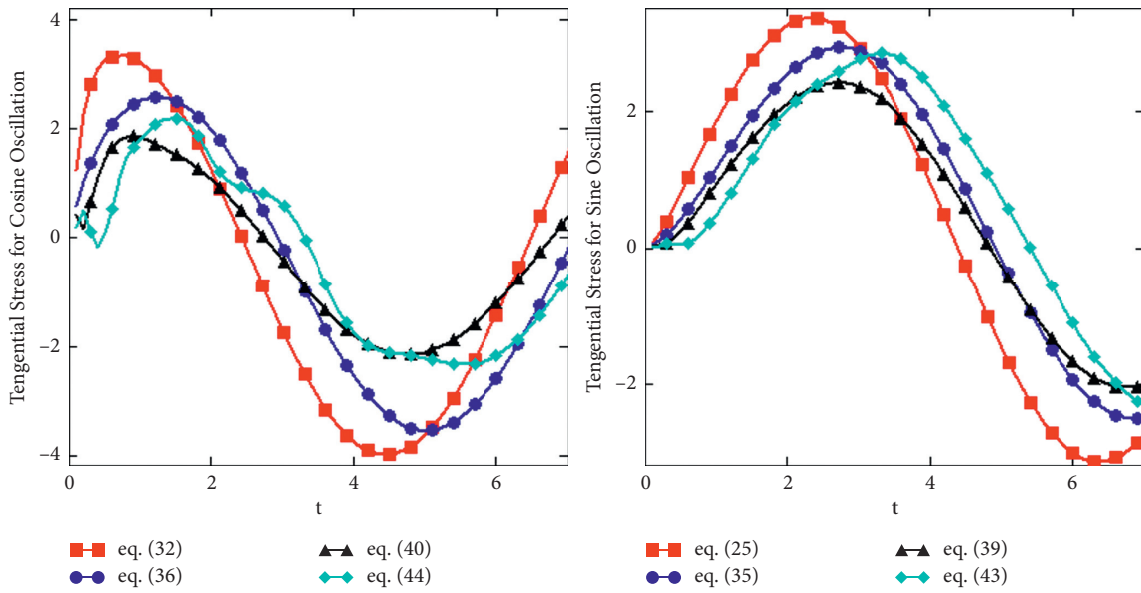

FIGURE 13: Tangential stresses of fractional Oldroyd-B fluid, classical Oldroyd-B fluid, fractional Maxwell fluid, and classical Maxwell fluid for both cos and sin.

TABLE 2: Comparison of analytical and numerical solution for velocity profile of sin oscillation.

t	λ_1	λ_2	α	β	Velocity (analytical)	Velocity (Stehfest's)	Velocity (Tzou's)
0.3					0.19679	0.19679	0.19698
0.6					0.49046	0.49044	0.49108
0.9					0.79985	0.79982	0.8005
	0.1				0.92838	0.92846	0.92026
	1				0.90133	0.90131	0.90187
	5				0.72345	0.72345	0.72371
		0.1			2.15514	2.15642	2.15508
		0.3			1.19366	1.19364	1.19391
		0.5			0.91705	0.91709	0.91542
			0.1		0.82248	0.82249	0.81367

TABLE 2: Continued.

t	λ_1	λ_2	α	β	Velocity (analytical)	Velocity (Stehfest's)	Velocity (Tzou's)
			0.5		0.83191	0.83194	0.82416
			0.9		0.84186	0.84194	0.83695
				0.2	0.7179	0.71795	0.71603
				0.5	0.72393	0.72382	0.72608
				0.7	0.72725	0.72696	0.73064

TABLE 3: Comparison of analytical and numerical solution for velocity profile of cos oscillation.

t	λ_1	λ_2	α	β	Velocity (analytical)	Velocity (Stehfest's)	Velocity (Tzou's)
0.3					1.10340	1.09977	1.05517
0.6					1.16489	1.16141	1.11978
0.9					1.11031	1.10694	1.06528
	0.1				1.11259	1.10913	1.07161
	1				1.1023	1.09865	1.05327
	5				1.09359	1.08982	1.03876
		0.1			1.77775	1.77494	1.68597
		0.3			1.26878	1.26496	1.19361
		0.5			1.09359	1.08982	1.03876
			0.1		1.1023	1.09865	1.05327
			0.5		1.1172	1.11542	0.92388
			0.9		1.2042	1.20333	1.23378
				0.2	1.03804	1.04065	0.98972
				0.5	1.08693	1.0851	0.88743
				0.7	1.10415	1.09827	0.95289

TABLE 4: Comparison of analytical and numerical solution for shear stresses of sin oscillation.

t	λ_1	λ_2	α	β	Shear stress (analytical)	Shear stress (Stehfest's)	Shear stress (Tzou's)
0.3					0.23055	0.23055	0.22853
0.6					0.49964	0.49965	0.49531
0.9					0.76883	0.76883	0.76204
	0.1				0.3223	0.3223	0.31942
	1				0.31801	0.31802	0.31525
	5				0.31444	0.31445	0.31178
		0.1			0.45165	0.45166	0.45033
		0.3			0.35301	0.35301	0.35062
		0.5			0.3194	0.3194	0.3166
			0.1		0.29581	0.29582	0.2927
			0.5		0.29495	0.294971	0.29309
			0.9		0.29711	0.29709	0.29765
				0.2	0.28779	0.28777	0.28832
				0.5	0.29213	0.29214	0.29181
				0.7	0.29412	0.29414	0.2924

TABLE 5: Comparison of analytical and numerical solution for shear stresses of cos oscillation.

t	λ_1	λ_2	α	β	Shear stress (analytical)	Shear stress (Stehfest's)	Shear stress (Tzou's)
0.3					0.99845	0.9926	0.76837
0.6					0.96564	0.95701	0.73931
0.9					0.85766	0.84791	0.6461
	0.1				0.99529	0.98762	0.77642
	1				0.97397	0.97164	0.7738
	5				0.9397	0.94018	0.81115
		0.1			1.45506	1.45601	1.40114
		0.3			1.17962	1.17937	1.03098

TABLE 5: Continued.

t	λ_1	λ_2	α	β	Shear stress (analytical)	Shear stress (Stehfest's)	Shear stress (Tzou's)
		0.5			1.0676	1.06564	0.87715
			0.1		1.47842	1.47583	1.36826
			0.5		1.41951	1.4202	1.41206
			0.9		1.32882	1.32841	1.31978
				0.2	1.25973	1.25822	1.28592
				0.5	1.409	1.40928	1.41688
				0.7	1.43243	1.43337	1.38511

6. Conclusion

This communication aims to provide exact solutions for the fractionalized Oldroyd-B fluid in a fluctuating quadrilateral duct by applying the discrete Laplace and double finite Fourier transforms. Also, a comparison is shown in tables for the analytical and numerical results. The corresponding results were not studied before and have important remarks concerning the prevailing equations for the nontrivial shear stress. These results fulfill all the executed initial and boundary conditions and were easily converted into parallel solutions. The parallel solutions for fractional Maxwell fluid, classical Oldroyd-B, and Maxwell fluid were regained as regulating case of the conventional solution. The following conclusions were drawn:

(i) Both sine and cosine oscillations of the velocity field decrease with the increase of fractional parameter α and vice versa for β

(ii) An increase in the values of λ_1 and λ_2 decreases the velocity profile of both sine and cosine oscillations

(iii) Dimensionless velocities comparison figured out fractional Oldroyd-B fluid is swiftest than fractional Maxwell fluid

(iv) Dimensionless shear stress changes behavior after half interval, and the opposite effect was seen between α and β fractional parameters

(v) Also, the analytical solutions show good agreement with the numerical results

In future, we will study, what will be the effects on fractional Oldroyd-B fluid via a fluctuating duct by adding the magnetic and porous factors.

Data Availability

No data were used to support the findings of this study.

Conflicts of Interest

The authors declare that they have no conflicts of interest.

References

[1] J. P. Hartnett and M. Kostic, "Heat transfer to Newtonian and non-Newtonian fluids in rectangular ducts," in *Advances in Heat Transfer* vol. 19, , pp. 247–356, Elsevier, 1989.

[2] G. G. Stokes, "On the effect of the rotation of cylinders and spheres about their axis in increasing the logarithmic decrement of the arc of vibration," 1886.

[3] K. R. Rajagopal, "Longitudinal and torsional oscillations of a rod in a non-Newtonian fluid," *Acta Mechanica*, vol. 49, no. 3, pp. 281–285, 1983.

[4] K. R. Rajagopal and R. K. Bhatnagar, "Exact solutions for some simple flows of an oldroyd-b fluid," *Acta Mechanica*, vol. 113, no. 1, pp. 233–239, 1995.

[5] A. Mahmood, N. A. Khan, I. Siddique, and S. Nazir, "A note on sinusoidal motion of a viscoelastic non-Newtonian fluid," *Archive of Applied Mechanics*, vol. 82, no. 5, pp. 659–667, 2012.

[6] T. Hayat, A. M. Siddiqui, and S. Asghar, "Some simple flows of an oldroyd-b fluid," *International Journal of Engineering Science*, vol. 39, no. 2, pp. 135–147, 2001.

[7] D. Valério, J. Machado, and V. Kiryakova, "Some pioneers of the applications of fractional calculus," *Fractional Calculus and Applied Analysis*, vol. 17, no. 2, pp. 552–578, 2014.

[8] C. Fetecau, "Analytical solutions for non-Newtonian fluid flows in pipe-like domains," *International Journal of Non-Linear Mechanics*, vol. 39, no. 2, pp. 225–231, 2004.

[9] N. D. Waters and M. J. King, "The unsteady flow of an elastico-viscous liquid in a straight pipe of circular cross section," *Journal of Physics D: Applied Physics*, vol. 4, no. 2, p. 204, 1971.

[10] W. P. Wood, "Transient viscoelastic helical flows in pipes of circular and annular cross-section," *Journal of Non-Newtonian Fluid Mechanics*, vol. 100, no. 1-3, pp. 115–126, 2001.

[11] S. S. Ray, A. Atangana, S. C. Noutchie, M. Kurulay, N. Bildik, and A. Kilicman, "Fractional calculus and its applications in applied mathematics and other sciences," *Mathematical Problems in Engineering*, vol. 2014, Article ID 849395, 2 pages, 2014.

[12] L. Debnath, "Recent applications of fractional calculus to science and engineering," *International Journal of Mathematics and Mathematical Sciences*, vol. 2003, no. 54, pp. 3413–3442, 2003.

[13] I. Podlubny, *Fractional Differential Equations: An Introduction to Fractional Derivatives, Fractional Differential Equations, to Methods of Their Solution and Some of Their Applications*, Elsevier, Amsterdam, Netherland, 1998.

[14] N Ali Shah and I. Khan, "Heat transfer analysis in a second grade fluid over and oscillating vertical plate using fractional caputo–fabrizio derivatives," *The European Physical Journal C*, vol. 76, no. 7, pp. 1–11, 2016.

[15] I. Khan, N. A. Shah, Y. Mahsud, and D. Vieru, "Heat transfer analysis in a maxwell fluid over an oscillating vertical plate using fractional caputo-fabrizio derivatives," *The European Physical Journal Plus*, vol. 132, no. 4, pp. 1–12, 2017.

[16] L. Debnath, *Transforms and Their Applications*, 2007.

[17] C. Fetecau and C. Fetecau, "The first problem of Stokes for an oldroyd-b fluid," *International Journal of Non-linear Mechanics*, vol. 38, no. 10, pp. 1539–1544, 2003.

[18] M. Jamil, N. A. Khan, and M. A. Imran, "New exact solutions for an oldroyd-b fluid with fractional derivatives: Stokes' first problem," *International Journal of Nonlinear Sciences and Numerical Stimulation*, vol. 14, no. 7-8, pp. 443–451, 2013.

[19] C. Fetecau, M. Nazar, and C. Fetecau, "Unsteady flow of an oldroyd-b fluid generated by a constantly accelerating plate between two side walls perpendicular to the plate," *International Journal of Non-Linear Mechanics*, vol. 44, no. 10, pp. 1039–1047, 2009.

[20] M. Kamran, M. Imran, M. Athar, and M. A. Imran, "On the unsteady rotational flow of fractional oldroyd-b fluid in cylindrical domains," *Meccanica*, vol. 47, no. 3, pp. 573–584, 2012.

[21] M. B. Riaz, M. A. Imran, and K. Shabbir, "Analytic solutions of oldroyd-b fluid with fractional derivatives in a circular duct that applies a constant couple," *Alexandria Engineering Journal*, vol. 55, no. 4, pp. 3267–3275, 2016.

[22] C. Fetecau and C. Fetecau, "Unsteady flows of oldroyd-b fluids in a channel of rectangular cross-section," *International Journal of Non-linear Mechanics*, vol. 40, no. 9, pp. 1214–1219, 2005.

[23] M. Nazar, F. Shahid, M. Saeed Akram, Q. Sultan, and Q. Sultan, "Flow on oscillating rectangular duct for maxwell fluid," *Applied Mathematics and Mechanics*, vol. 33, no. 6, pp. 717–730, 2012.

[24] H. I. Ghada and A. M. Abdulhadi, "Flow through an oscillating rectangular duct for generalized oldroyd-b fluid with fractional derivatives," *IOSR Journal of Mathematics*, vol. 10, no. 5, 2014.

[25] S. Wang, P. Li, and M. Zhao, "Analytical study of oscillatory flow of maxwell fluid through a rectangular tube," *Physics of Fluids*, vol. 31, no. 6, Article ID 063102, 2019.

[26] X. Sun, S. Wang, and M. Zhao, "Oscillatory flow of maxwell fluid in a tube of isosceles right triangular cross section," *Physics of Fluids*, vol. 31, no. 12, Article ID 123101, 2019.

[27] A. Farooq, M. Kamran, Y. Bashir, H. Ahmad, A. Shahzad, and Y.-M. Chu, "On the flow of MHD generalized maxwell fluid via porous rectangular duct," *Open Physics*, vol. 18, no. 1, pp. 989–1002, 2020.

[28] Q. Sultan, M. Nazar, U. Ali, and M. Imran, "Unsteady flow of oldroyd-b fluid through porous rectangular duct," *International Journal of Nonlinear Science*, vol. 15, no. 3, pp. 195–211, 2013.

[29] S. Wang and M. Zhao, "Analytical solution of the transient electro-osmotic flow of a generalized fractional maxwell fluid in a straight pipe with a circular cross-section," *European Journal of Mechanics-B: Fluids*, vol. 54, pp. 82–86, 2015.

[30] X. Guo and H. Qi, "Analytical solution of electro-osmotic peristalsis of fractional jeffreys fluid in a micro-channel," *Micromachines*, vol. 8, no. 12, p. 341, 2017.

[31] X. Wang, H. Qi, B. Yu, Z. Xiong, and H. Xu, "Analytical and numerical study of electroosmotic slip flows of fractional second grade fluids," *Communications in Nonlinear Science and Numerical Simulation*, vol. 50, pp. 77–87, 2017.

[32] A. U. Awan, M. D. Hisham, and N. Raza, "The effect of slip on electro-osmotic flow of a second-grade fluid between two plates with caputo–fabrizio time fractional derivatives," *Canadian Journal of Physics*, vol. 97, no. 5, pp. 509–516, 2019.

[33] N. A. Shah, X. Wang, H. Qi, S. Wang, and H. Ahmad, "Transient electro-osmotic slip flow of an oldroyd-b fluid with time-fractional caputo-fabrizio derivative," *Journal of Applied and Computational Mechanics*, vol. 5, no. 4, pp. 779–790, 2019.

[34] B. Wang, M. Tahir, M. Imran, M. Javaid, and C. Y. Jung, "Semi analytical solutions for fractional oldroyd-b fluid through rotating annulus," *IEEE Access*, vol. 7, pp. 72482–72491, 2019.

[35] M. Kamran, Y. Bashir, A. Farooq et al., "Study on the helicoidal flow through cylindrical annuli with prescribed shear stresses," *Results in Physics*, vol. 23, Article ID 103993, 2021.

[36] J. G. Oldroyd, "On the formulation of rheological equations of state," *Proceedings of the Royal Society of London-Series A: Mathematical and Physical Sciences*, vol. 200, pp. 523–541, 1950.

[37] S. C. Pandey, "The Lorenzo-Hartley's function for fractional calculus and its applications pertaining to fractional order modelling of anomalous relaxation in dielectrics," *Computational and Applied Mathematics*, vol. 37, no. 3, pp. 2648–2666, 2018.

[38] M. Nazar, M. Zulqarnain, M. Saeed Akram, and M. Asif, "Flow through an oscillating rectangular duct for generalized maxwell fluid with fractional derivatives," *Communications in Nonlinear Science and Numerical Simulation*, vol. 17, no. 8, pp. 3219–3234, 2012.